

Determination of the nature of fluctuations using ^8Li and ^9Li β -NMR and spin-lattice relaxationA. Chatzichristos,^{1,2,*} R. M. L. McFadden,^{2,3} V. L. Karner,^{2,3} D. L. Cortie,^{1,2,3} C. D. P. Levy,⁴ W. A. MacFarlane,^{2,3} G. D. Morris,⁴ M. R. Pearson,⁴ Z. Salman,⁵ and R. F. Kiefl^{1,2,4}¹*Department of Physics and Astronomy, University of British Columbia, Vancouver, British Columbia, Canada V6T 1Z1*²*Stewart Blusson Quantum Matter Institute, University of British Columbia, Vancouver, British Columbia, Canada V6T 1Z4*³*Department of Chemistry, University of British Columbia, Vancouver, British Columbia, Canada V6T 1Z4*⁴*TRIUMF, 4004 Wesbrook Mall, Vancouver, British Columbia, Canada V6T 2A3*⁵*Laboratory for Muon Spin Spectroscopy, Paul Scherrer Institute, CH-5232 Villigen PSI, Switzerland*

(Received 26 March 2017; published 31 July 2017)

We report a comparison of the $1/T_1$ spin-lattice relaxation rates for ^9Li and ^8Li in Pt and SrTiO_3 , in order to differentiate between magnetic and electric quadrupolar relaxation mechanisms. In Pt, the ratio of the $1/T_1$ spin relaxation rates R_{Pt} was found to be 6.82(29), which is close to but less than the theoretical limit of ~ 7.68 for pure magnetic relaxation. In SrTiO_3 this ratio was found to be 2.7(3), which is close to but larger than the theoretical limit of ~ 2.14 expected for pure electric quadrupolar relaxation. These results bring insight into the nature of the fluctuations in the local environment of implanted ^8Li observed by β -NMR.

DOI: [10.1103/PhysRevB.96.014307](https://doi.org/10.1103/PhysRevB.96.014307)**I. INTRODUCTION**

^8Li β -detected NMR (β -NMR) has been established as a powerful tool for materials science due to its inherent sensitivity to magnetic and electronic properties [1]. The principal success of TRIUMF's low-energy incarnation of β -NMR [2,3] is the ability to study thin films, surfaces, and interfaces, where conventional NMR is difficult or impossible. This stems from β -NMR's high sensitivity relative to conventional NMR; for β -NMR typically only $\sim 10^8$ nuclei (instead of $\sim 10^{17}$) are required for a signal. The only other real-space technique with equivalent sensitivity over a comparable material length scale (viz., 10–200 nm) [4] is low-energy muon spin rotation (LE- μ SR) [5]; however, it operates in a complementary time window due to the different probe lifetimes (1.21 s for $^8\text{Li}^+$ vs 2.2 μs for μ^+). Thus, both techniques have leveraged the nuclear physics of beta decay to investigate topical problems in condensed matter physics, including magnetic surfaces, thin film heterostructures, topological insulators, superconductors, etc.

A key issue in any ^8Li β -NMR experiment is to identify the source of spin-lattice relaxation (SLR) and in particular whether the fluctuations driving the SLR are magnetic or electric in origin. Unlike the positive muon, μ^+ ($I = 1/2$), ^8Li ($I = 2$) is *not* a pure magnetic probe and its relaxation is sensitive to both fluctuating magnetic fields and electric field gradients (EFGs). In some cases, the primary source of relaxation may be inferred. For example, in simple metals the observed relaxation is linear in temperature [6], as expected from the Korringa relaxation [7], which originates from a magnetic hyperfine interaction between the nuclear spin and the spin of the conduction electrons. However, in more complicated instances, such as heterostructures comprising magnetic and nonmagnetic layers, it becomes difficult to determine the contribution of each type of relaxation. $\text{LaAlO}_3/\text{SrTiO}_3$ multilayers are particularly illustrative of this point; the bulk layers are nonmagnetic insulators, while there is evidence of magnetism at their interfaces [8].

In conventional NMR it is possible to differentiate between relaxation mechanisms by isotopic variation of the nuclear probe, since the absolute relaxation rates for each isotope scale according to their nuclear moments. For two isotopes with significantly different nuclear moments (e.g., ^6Li and ^7Li [9]) the ratio of the relaxation rates should be distinctly different in the limits of either pure magnetic or pure electric quadrupolar relaxation. In this paper, we test the feasibility of isotope comparison applied to β -NMR, using ^8Li and ^9Li , two β -radioactive isotopes. The stopping sites of ^8Li and ^9Li are often interstitial rather than substitutional as in the case of conventional NMR. However, we expect that both implanted ^8Li and ^9Li will probe the same sites. Measurements on ^9Li are more time consuming than those for ^8Li . This is related to the fact that ^9Li lies one neutron further away from the valley of stability, consequently the beam intensity in this experiment was about ten times lower for ^9Li than for ^8Li , and has a more complicated β -decay scheme, which results in a β -decay asymmetry for ^9Li about three times smaller than for ^8Li , as will be discussed below.

Measurements reported here were made in Pt metal, where the spin relaxation rate of ^8Li (^9Li) is dominated by Korringa scattering [10], which is magnetic, and in strontium titanate (SrTiO_3), which is a nonmagnetic insulator with a large static electric quadrupolar interaction for implanted ^8Li . SrTiO_3 is a common substrate material but also has interesting properties on its own which have been studied extensively with a wide variety of methods, including β -NMR. Although we expect the quadrupolar fluctuations in EFG causing spin relaxation to dominate, there are also potential magnetic sources of relaxation that could contribute, as explained below.

In the following sections we first summarize the theoretical considerations behind β -NMR, as well as the isotopic variation method. This is then followed by a description of the experiment, and finally we present the experimental results along with a discussion.

II. THEORY

The basis of β -NMR is the parity-violating weak interaction, whereby the direction of the emitted electron (positron)

*aris.chatzichristos@alumni.ubc.ca

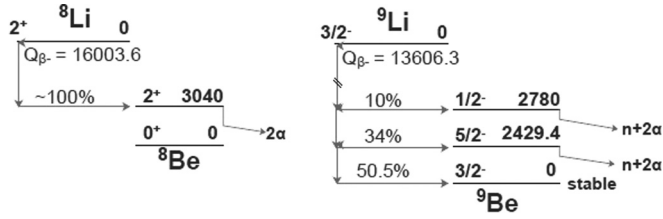


FIG. 1. Properties of the principle β -decay modes of ${}^8\text{Li}$ and ${}^9\text{Li}$ [11]. The asymmetry (a) of each decay mode of ${}^9\text{Li}$ is documented in Table I. The total asymmetry for ${}^9\text{Li}$ is the sum of the asymmetry weighted by the relevant probability of each decay mode.

from the decaying nucleus is correlated with the nuclear spin polarization at the time of decay,

$$W(\theta) = 1 + \beta a p \cos(\theta), \quad (1)$$

where $\beta = v/c$ is the velocity of the high-energy electron (positron) normalized to the speed of light, p is the magnitude of the nuclear polarization vector, θ is the angle between the nuclear polarization and the electron (positron) velocity, and a is the asymmetry parameter depending on the properties of nuclear β decay. The theory of nuclear beta decay predicts that a is about $1/3$ for ${}^8\text{Li}$ and considerably smaller (~ 0.1) for ${}^9\text{Li}$ [11], if averaged over all the decay modes.

The reduction in asymmetry for ${}^9\text{Li}$ compared to ${}^8\text{Li}$ is attributed to ${}^9\text{Li}$'s more complicated β -decay scheme. In particular, ${}^9\text{Li}$ has three main decay channels, two of which have opposite asymmetries that nearly cancel after weighting by the branching probabilities. Thus, most of the observed asymmetry is from the weakest decay mode, which has a branching probability of only 0.1 but a large theoretical asymmetry parameter $a = 1.0$. The relevant branching probabilities and asymmetries of each decay mode are reported in Fig. 1. We note in passing that it should be possible to enhance the β -NMR signal from ${}^9\text{Li}$ by tagging events according to whether or not an α is emitted, which will allow us to distinguish between the different decay channels and isolate their contributions. This is currently being explored as a way to optimize the β -NMR of ${}^9\text{Li}$.

The resulting anisotropic decay pattern for the high-energy electron (positron) allows one to monitor the nuclear polarization from highly polarized ${}^8\text{Li}^+$ or ${}^9\text{Li}^+$ beams implanted in the sample. In particular, the asymmetry in the count rate at time t between two opposing beta detectors is proportional to the component of nuclear polarization along the direction defined by the two detectors,

$$A(t) = \frac{N_B(t) - N_F(t)}{N_B(t) + N_F(t)} = A_0 p_z(t), \quad (2)$$

TABLE I. The asymmetry (a) of each decay mode of ${}^9\text{Li}$ in Fig. 1.

${}^9\text{Be}$ state	Probability	I^π	a	Decay mode
Ground state	50.5%	$3/2^-$	$-2/5$	Stable
2429.4 MeV	34%	$5/2^-$	$3/5$	$n + 2\alpha$
2780 MeV	10%	$1/2^-$	-1	$n + 2\alpha$

where $N_B(t)$ and $N_F(t)$ are the counts measured in the backward and forward detectors, $p_z(t)$ is the component of nuclear polarization along the z axis defined by the detectors, and t is the time of decay after implantation. The detectors are generally positioned so that z is along the direction of initial polarization. Note that the asymmetry in the count rate has a maximum value of A_0 at $t = 0$ which is reduced relative to the theoretical asymmetry a , as calculated from the nuclear properties, owing to instrumental effects such as the finite solid angle subtended by the detectors and scattering of the betas before reaching the detectors. Note also that $p_z(t)$ and thus $A(t)$ are time dependent, reflecting the fact that the nuclear polarization is subject to spin relaxation processes in the sample, which in fact is the quantity of interest in this experiment.

Information on the fluctuations of the electromagnetic fields in a material of interest is obtained through measurements of the spin-lattice relaxation (SLR) rate in the absence of a rf magnetic field. The SLR may be studied by implanting a series of beam pulses into the sample and then monitoring $\mathcal{A}(t)$, which is the convolution of $A(t - t')$ with the beam pulse $N(t')$, where t' is the time of arrival for given probe and $t - t'$ is the time spent in the sample before its beta decay,

$$\mathcal{A}(t) = \int_{-\infty}^t N(t') A(t - t') dt'. \quad (3)$$

In general, the SLR rate, usually denoted as $1/T_1$ (with T_1 being the longitudinal spin-lattice relaxation time), originates from fluctuations in the local environment arising from fundamental processes, such as phonon scattering, magnon scattering, conduction electron scattering, diffusion, etc. The total observed rate can be decomposed into a sum of individual contributions, which may be grouped into magnetic ($1/T_1^M$) and electric quadrupolar ($1/T_1^Q$) terms,

$$\frac{1}{T_1} = \frac{1}{T_1^M} + \frac{1}{T_1^Q}. \quad (4)$$

Most often one of the relaxation mechanisms will dominate. For instance, we expect Korringa relaxation to be dominant in simple metals.

The magnitudes of each contribution for a given probe nucleus scale according to their nuclear properties, namely, their spin I , magnetic moment μ , and electric quadrupole moment Q . Measurements of SLR rates for two different isotopes under identical experimental conditions (i.e., magnetic field, temperature, etc.) can be compared through their ratio R ,

$$R(I, I') \equiv \frac{1/T_1(I)}{1/T_1(I')} = \frac{1/T_1^M(I) + 1/T_1^Q(I)}{1/T_1^M(I') + 1/T_1^Q(I')}, \quad (5)$$

where I and I' denote the spin quantum number of each isotope. Two limits are of interest here: when the relaxation is *solely* due to either magnetic or quadrupolar interactions within the host sample. In the former case, Eq. (5) reduces to the ratio of pure magnetic relaxation R_M , which in the limit of fast fluctuations (i.e., $\tau_c^{-1} \gg \omega_0$, where τ_c is the NMR correlation time and ω_0 is the Larmor resonance frequency) is

$$R_M(I, I') = \left(\frac{\mu/I}{\mu'/I'} \right)^2 = \left(\frac{\gamma}{\gamma'} \right)^2, \quad (6)$$

TABLE II. Intrinsic nuclear properties of Li radioisotopes used in β -NMR and β -NQR. I^π is the nuclear spin (and parity), μ is the magnetic moment, and Q is the electric quadrupole moment.

	I^π	τ_β (s)	μ (μ_N) ^a	Q (mb) ^b
⁸ Li	2 ⁺	1.2096(5) [14]	+1.653560(18) [15]	+32.6(5) [16]
⁹ Li	3/2 ⁻	0.2572(6) [17]	+3.43678(6) [15]	-31.5(5) [16]

^aThe magnetic moments have been corrected for diamagnetic shielding.

^bThe quadrupole moments were determined from their ratios, starting with the well-known value for ⁷Li [13].

where μ and γ are the magnetic moment and gyromagnetic ratio of each isotope. Note that the fast fluctuation limit ensures that $1/T_1$ is independent of ω_0 .

In the other case, Eq. (5) yields the ratio of relaxation rates in the pure quadrupolar limit R_Q ,

$$R_Q(I, I') = \frac{f(I)}{f(I')} \left(\frac{Q}{Q'} \right)^2, \quad (7)$$

where Q are the nuclear quadrupole moments, and [12]

$$f(I) = \frac{2I + 3}{I^2(2I - 1)}. \quad (8)$$

Thus, given the nuclear moments of each isotope, one can calculate the ratio of relaxation rates when either mechanism is dominant. Using Eqs. (6) and (7), along with the nuclear spins and moments for ⁸Li and ⁹Li (see Table II), we find the limiting cases for $T_1^{-1}({}^9\text{Li})/T_1^{-1}({}^8\text{Li})$: 7.679 64(16) and 2.1362(4) for R_M and R_Q , respectively. The difference between these limits is not as pronounced as for ⁶Li and ⁷Li [9], where R_M and R_Q differ by a factor of ~ 90 [13]. Nevertheless, ⁸Li and ⁹Li are sufficiently different that the nature of fluctuations and resulting spin relaxation (magnetic versus electric quadrupolar) may be differentiated by such a comparison.

III. EXPERIMENT

The experiment was performed using 18 keV beams of ⁸Li⁺ and ⁹Li⁺ at TRIUMF's Isotope Separator and Accelerator Facility (ISAC) in Vancouver, Canada. ISAC is capable of providing an intense beam for a large number of isotopes of various elements [18], including ⁸Li and ⁹Li. For this experiment, TRIUMF's dedicated β -NMR and β -NQR spectrometers were used. A detailed discussion on the characteristics of the spectrometers can be found elsewhere [3,19].

Before reaching the spectrometer, the Li⁺ ion beam first passes through the ISAC polarizer [2]. The first stage of the polarizer is to neutralize the beam by passing it through a Rb vapor cell. The neutral beam then drifts ~ 2 m during which time the ${}^2S_{1/2}$ - ${}^2P_{1/2}$ optical D_1 transition is pumped with circularly polarized laser light. The last stage is to reionize the beam in a He gas so that the polarized beam can be delivered alternately to the spectrometers. Previous work shows that the nuclear polarization of the beam after stopping in the sample is $\sim 70\%$ [20].

It is important to note that unlike conventional NMR, where the Boltzmann factor determines the polarization, the nuclear polarization in β -NMR is close to unity and independent of the sample temperature and magnetic field. Consequently, measurements can be made under conditions where conventional NMR is difficult or impossible, e.g., at high temperatures, low magnetic fields, or in thin films. The intensity of the implanted beam (typically $\sim 10^7$ s⁻¹) is such that the concentration of the nuclear probes is so small that there is no interaction between probes and thus no homonuclear spin coupling.

IV. RESULTS AND DISCUSSION

To demonstrate the comparison of ⁸Li and ⁹Li in β -NMR, two very different materials were selected. The first is Pt, which is a d -band metal in which the ⁸Li resides at a site with little or no quadrupolar interaction. In this test case we expect the relaxation to be predominantly magnetic, originating from Korringa scattering. SrTiO₃, on the other hand, is a nonmagnetic insulator with few nuclear moments. Previous work in SrTiO₃ shows that ⁸Li experiences a large quasistatic quadrupolar interaction [21]. Thus in this case we expect quadrupole fluctuations to play a more important role. Nevertheless, it is still unclear to what extent magnetic effects can be neglected in SrTiO₃. For example, O vacancies in SrTiO₃ result in two Ti³⁺ ions which are typically paramagnetic. In principle, the resulting paramagnetic defects would have low-frequency magnetic fluctuations which will contribute to the SLR of the implanted Li nucleus in SrTiO₃.

A. Platinum

The sample was a high-purity (99.999%) Pt foil with dimensions 12×12 mm² and thickness of 0.1 mm. It was cut from the same initial foil that was studied by Ofer *et al.* [10].

⁸Li⁺ resonance measurements in Pt have shown a single narrow line below 300 K, indicating that ⁸Li⁺ occupies a single site with a vanishing (static) EFG [22,23]. The spectrum is also simpler than in other metals, where multiple Li⁺ sites are found below 300 K [24–30].

Given the simplicity of the resonance spectrum, we expect SLR in Pt to follow a single exponential form with

$$A(t - t') = \exp[-\lambda(t - t')/T_1]. \quad (9)$$

Substituting this into Eq. (3) and assuming a square beam pulse during the time interval $[0, \Delta]$, one obtains a form for the asymmetry during and after the pulse given by

$$\mathcal{A}(t) = \begin{cases} A_0 \frac{\tau'}{\tau_\beta} \frac{1 - \exp(-t/\tau')}{1 - \exp(-t/\tau_\beta)}, & t \leq \Delta, \\ A(\Delta) \exp[-(-t - \Delta)/T_1], & t > \Delta, \end{cases} \quad (10)$$

where τ_β is the radioactive lifetime, $1/\tau' = 1/\tau_\beta + 1/T_1$, and A_0 is the initial asymmetry at the time of implantation. Note that the SLR spectrum has two distinct regions (see Fig. 2): During the beam pulse ($0 < t < \Delta$) the asymmetry relaxes towards a dynamic equilibrium value [6],

$$\bar{\mathcal{A}} = \frac{A_0}{1 + \tau_\beta/T_1}, \quad (11)$$

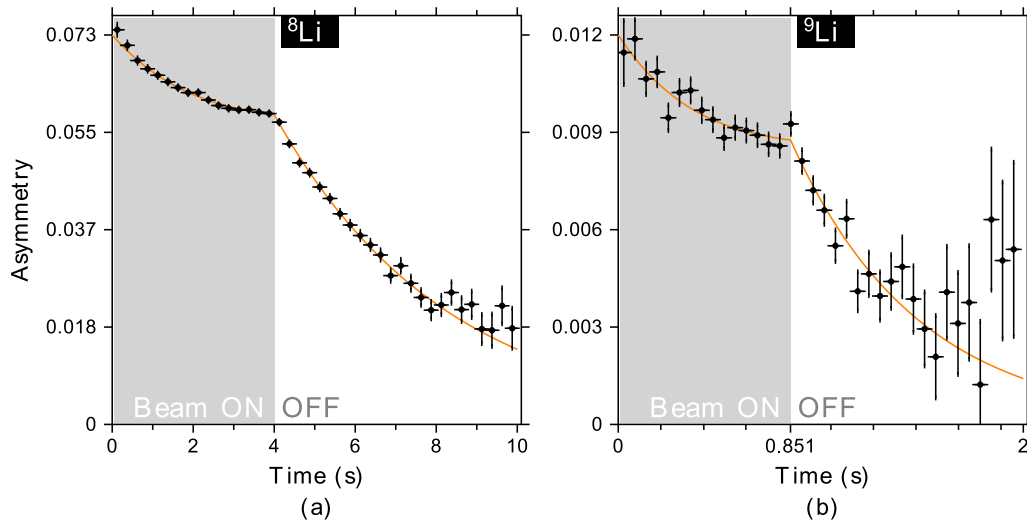


FIG. 2. SLR spectra for $^8\text{Li}^+$ (left) and $^9\text{Li}^+$ (right) implanted in Pt foil with an energy of 18 keV at 300 K under 6.55 T. The solid lines are fits to Eq. (10). Note the different time scales, which reflect the lifetime of each radionuclide. The absolute SLR rate for $^9\text{Li}^+$ is 1.60(10) and 0.2368(26) for $^8\text{Li}^+$.

whereas after the beam pulse ($t > \Delta$) $\mathcal{A}(t)$ decays towards the Boltzman equilibrium value, which is essentially zero on our scale. Note the pronounced kink in $\mathcal{A}(t)$ at $t = \Delta$ when the beam pulse ends. This is also the time with the highest event rate and smallest statistical uncertainty in $\mathcal{A}(t)$. For both isotopes the length of the beam pulse ($\sim 3.3\tau_\beta$) and the total observation time ($\sim 9.9\tau_\beta$) were chosen to minimize the statistical uncertainties.

The SLR rates for $^8\text{Li}^+$ and $^9\text{Li}^+$ implanted at 300 K were measured in magnetic fields of 1.90 and 6.55 T, the latter being shown in Fig. 2. Several general distinctions should be pointed out between SLR spectra for $^8\text{Li}^+$ and $^9\text{Li}^+$ in Pt: The initial asymmetry (i.e., A_0) for $^8\text{Li}^+$ is ~ 6 times greater than for $^9\text{Li}^+$; $1/T_1$ is ~ 7 times larger for $^9\text{Li}^+$ than for $^8\text{Li}^+$; and the relative uncertainty of the SLR rate measurements for $^9\text{Li}^+$ is greater by a factor of ~ 5 than for $^8\text{Li}^+$. The latter can be understood as follows: The statistical figure of merit for any β -NMR measurement is A^2N , where A is the observable asymmetry and N is the total number of decay events—both factors for ^9Li are significantly reduced relative to ^8Li . Since ^9Li lies farther away from the valley of nuclear stability, it has a shorter half-life and fewer ions are extracted from the ion source and delivered to the spectrometer (here, $\sim 10^6 \text{ s}^{-1}$ vs $\sim 10^7 \text{ s}^{-1}$ for $^8\text{Li}^+$). This in turn reduces the factor N for ^9Li . Also, as explained above, the asymmetry for ^9Li is much smaller than for ^8Li . As a result, about 90% of the data acquisition was spent on ^9Li , since these results dominated our uncertainty in the ratio of the relaxation rates.

Temperature-dependent SLR of $^8\text{Li}^+$ in Pt has been studied previously by Ofer *et al.* [10] between 3 and 295 K at 4.10 T, where the SLR rate was found to increase linearly with temperature, implying Korringa relaxation [7]. This relation holds for high magnetic fields and different implantation energies. The temperature-dependent $^8\text{Li}^+$ SLR rates at various magnetic fields are shown in Fig. 3, including our measurements, as well as results on Pt foil by Ofer *et al.* [10]. The ^8Li SLR rate at 6.55 T is in good agreement with the Korringa fit by Ofer *et al.* [10], extrapolated to 300 K, whereas the measured SLR

rate at 1.9 T is lower by about 10%. It is unlikely that this is a real effect since any additional source of relaxation would *increase* the relaxation at the lower magnetic field, which is opposite to what is observed. The slight reduction in $1/T_1$ measured at 1.9 T suggests there may be a small systematic error related to the fact that the beam spot is a bit larger and the ratio between the beta rates in the two detectors is different compared to the higher field. However, it should be noted that the measured ^8Li SLR rates in Pt foil appear to increase linearly with temperature, independent of implantation energy and applied magnetic field.

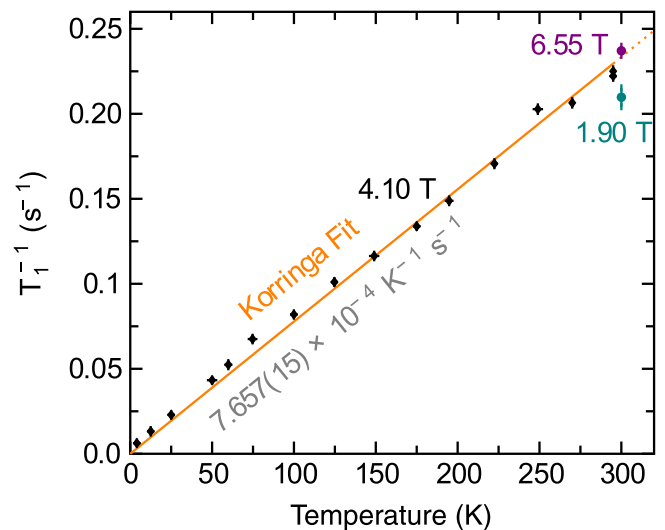


FIG. 3. Measured SLR rates for ^8Li implanted in Pt. The relaxation rate increases linearly with temperature, appearing insensitive to both implantation energy and magnetic field strength, consistent with a Korringa mechanism [7]. Measurements from this work are highlighted in colored disks, while black diamond markers indicate data from earlier measurements on Pt foil [10]. The solid line is a Korringa fit to *all* the SLR rates in Pt and differs somewhat from the result of Ofer *et al.* [10] due to the additional data points from this work.

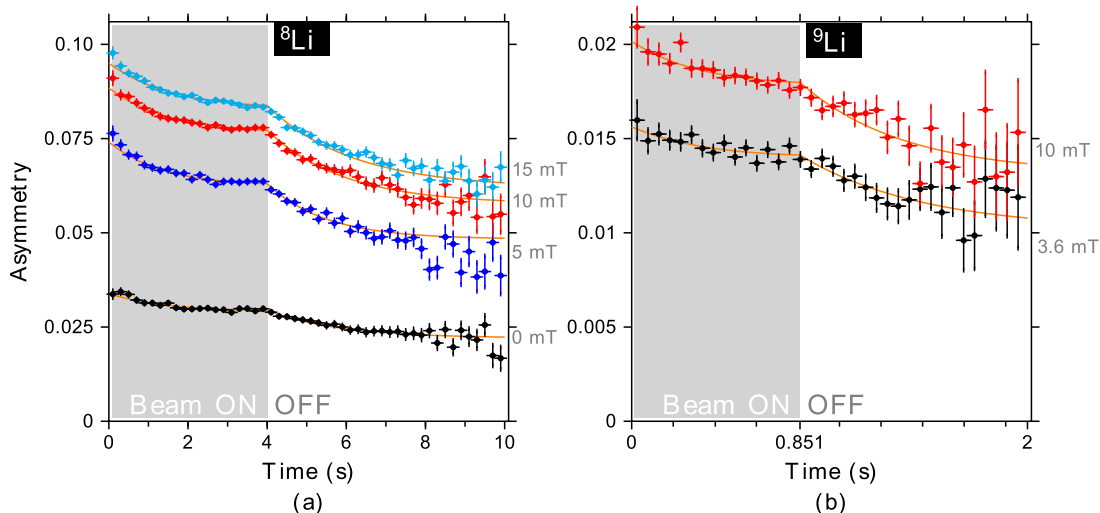


FIG. 4. SLR spectra of ^8Li (left) and ^9Li (right) in single-crystal SrTiO_3 at 300 K. The solid lines are a global fit to Eqs. (3) and (12) where a common parameter f is shared between all spectra.

The ratios of $T_1^{-1}(^9\text{Li})/T_1^{-1}(^8\text{Li})$ at 6.55 and 1.90 T are in good agreement with each other and we find a relaxation rate ratio R_{Pt} of 6.8(4) and 5.9(9) at 6.55 and 1.90 T, respectively.

B. Strontium titanate

SrTiO_3 was chosen for this study since it is a nonmagnetic insulator, and a material where the ^8Li relaxation is expected to be dominated by quadrupolar fluctuations. It has been studied extensively with low-energy ^8Li β -NMR [31–33]. SrTiO_3 is a cubic perovskite at 300 K. Implanted ^8Li occupies three equivalent interstitial noncubic sites [34], namely, the face-centered sites in the unit cell centered at Sr^{2+} . At 300 K, the EFG is axially symmetric, with the main axis along Sr - ^8Li - Sr .

Two SrTiO_3 samples were studied in this experiment. Both were $10 \times 8 \times 0.5 \text{ mm}^3$ single crystals with (100) orientation. Both samples were epitaxially polished (0.2 nm rms roughness). Sample S1 was left bare, while sample S2 was capped with 30 nm of LaTiO_3 [35]. At the implantation energy of 18 keV, a negligible fraction of $^8\text{Li}^+$ ions stop in the LaTiO_3 film, or the near-surface region. This was checked for both ^8Li and ^9Li by using SRIM 2013 [36].

Figure 4 shows the SLR spectra for ^8Li and ^9Li at 300 K at various magnetic fields between 0 and 15 mT applied along a (100) cubic crystallographic axis. It is evident from the data that the relaxation is more complex than in Pt since a single exponential fails to describe the decay of spin polarization.

The spectra were best fitted with a two-component exponential function, but given that one of the relaxation rates is found to be nearly zero, a phenomenological relaxation function of the following form [33] was used,

$$A(t - t') = f \exp[-\lambda(t - t')] + (1 - f), \quad (12)$$

where f is the fraction of the relaxing asymmetry ($0 \leq f \leq 1$) and $\lambda \equiv 1/T_1$.

Since f is approximately field independent in our range of fields, the SLR spectra for ^8Li and ^9Li were fit globally, sharing a common f , which turned out to be 0.347(3). As f was about the same in zero field (ZF), the more complex relaxation function observed in SrTiO_3 must be unrelated to the angle between

the magnetic field and the symmetry axis of the EFG. Consequently, there must be an additional source of fluctuations affecting the SLR for all three sites in the same way but in an inhomogeneous manner either in time or space. Previous studies have found that the relaxing fraction f is also temperature independent [33]. This suggests that the origin of the relaxing component should be structural, associated with defects close to about one third of the implanted Li, with the rest being in a nonrelaxing environment away from such centers.

Regarding the relaxation function, note that this is an unfamiliar regime, where the Zeeman interaction is smaller than $\nu_Q = 153.2 \text{ kHz}$ over the full range of fields, since even for our highest-field measurement at 15 mT, $\gamma B = 94 \text{ kHz}$. At high fields (several T), previous work suggests that $f = 0$ [21]. In the high-field limit, the relaxation of any β -NMR experiment approaches zero, because the Zeeman splitting becomes larger than the fluctuation rate terms giving rise to relaxation, which in turn converts the relaxing component into a nonrelaxing one, leading to $f = 0$.

The SLR rate for ^8Li is found to vary weakly with applied magnetic field below 15 mT, reaching a plateau below 5 mT (see Fig. 5). It is likely, but unclear due to the limited statistics, that a similar behavior occurs for ^9Li . At 300 K, the ratio of the $^9\text{Li}/^8\text{Li}$ SLR rates for SrTiO_3 , R_{STO} , was found to be 3.7(7) at 10 mT and 2.4(5) at 3.6 mT.

For comparison, the SLR rate of ^8Li and ^9Li was also measured in a second SrTiO_3 sample (S2). These spectra were fitted globally with the same fitting function as in the first SrTiO_3 sample. The shared relaxing fraction in this case was 0.341(2), very close to the value calculated independently from the other SrTiO_3 sample. The ratio of relaxation rates in this sample at 10 mT was found to be 2.4(5).

C. Ratio of relaxation rates

The ratio of relaxation rates in platinum $R_{\text{Pt}} = 6.82(29)$, which is the weighted average of the measurements at 6.55 and 1.90 T. Note that this value is somewhat less than expected from the pure magnetic limit R_{M} (Fig. 6).

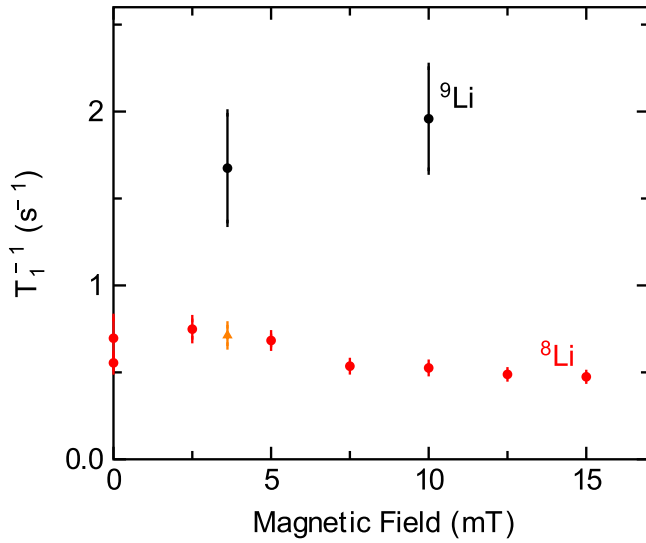


FIG. 5. Field dependence of $1/T_1$ for ^8Li and ^9Li in SrTiO_3 at 300 K. The (orange) triangle represents a linear interpolation at 3.6 mT from the 2.5 and 5 mT ^8Li measurements.

The reason for this discrepancy could be the nonzero temperature. All measurements were taken at 300 K where the lithium ions could have some quadrupolar contribution due to local vibrations and scattering of phonons which leads to a fluctuating EFG. However, $1/T_1$ is very linear in temperature, whereas any such contributions would have a stronger temperature dependence. It would be interesting to repeat the measurements at a lower temperature to check whether or not R_{Pt} is closer to the magnetic limit. In principle, the scattering of electrons at the Fermi surface, which is responsible for Korringa relaxation (see Fig. 3), could also produce a fluctuating EFG and a linear temperature dependence $1/T_1$, which is electric quadrupolar in origin.

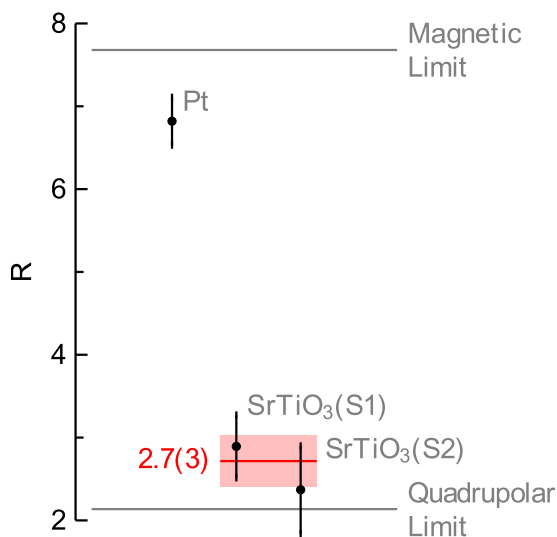


FIG. 6. Ratios of ^9Li to ^8Li $1/T_1$ relaxation rates in Pt (weighted average of all measurements) and in the two SrTiO_3 samples. The red line represents the weighted average of the measurements in both SrTiO_3 samples.

However, we could not find any calculations of this effect. In any case, an electric quadrupolar contribution to $1/T_1$ cannot be very large in Pt at 300 K.

We also reported a value of R_{STO} in two samples of SrTiO_3 . In the first sample, the weighted average R_{STO} of the measurements at 3.6 and 10 mT yielded 2.9(4). This value is close, but not within experimental error, of the quadrupolar limit of $R_Q \approx 2.14$. After taking into account the measurement on the second SrTiO_3 sample, which was 2.4(5) at 10 mT, the weighted ratio of relaxation rates in SrTiO_3 is found to be 2.7(3), closer to the quadrupolar limit. Still, there is a small disagreement which suggests some small magnetic contribution to $1/T_1$.

This small magnetic relaxation may be related to the observed nonexponential decay of polarization. The relaxing fraction f has been found in previous studies as well and it is approximately temperature independent [33] and independent of the angle between the magnetic field and the crystallographic axis [37]. This suggests that it could be due to the dynamics associated with defects close to some of the implanted Li. These fluctuations would be primarily paraelectric [37], but a small portion could be magnetic in origin. For example, any O vacancies a few lattice sites away would give rise to paramagnetic Ti^{3+} ions, in addition to paraelectric fluctuations. A typical level of oxygen vacancies in SrTiO_3 of about 1%–2% would result in lithium having such a defect for a nearest or next-nearest neighbor 20%–30% of the time, which could explain the fraction $f \sim 0.3$.

As to whether these defects are primarily intrinsic to the crystal or caused by the beam implantation, note the following: There is no doping taking place with ^8Li , since each ion decays into a beta and two alphas. ^9Li , on the other hand, decays into the stable ground state of ^9Be half of the time, so some Be doping should be expected. This doping is calculated to be in the order of parts per billion (50 ppb for Pt, 130 ppb for SrTiO_3). Such a small concentration should not create any considerable effect.

In addition, the implantation of a typical lithium ion can create multiple Frenkel pairs. Using SRIM, the upper boundary of their concentration was calculated in the order of 100 ppm in SrTiO_3 and ~ 50 ppm in Pt. Note that these defects would be formed gradually with time, i.e., they would affect primarily the measurements taken last. Such time dependence was not observed, though.

In comparison, the intrinsic defects in SrTiO_3 (primarily O vacancies) are in the $\sim 1\%$ range, orders of magnitude higher than even the upper limit of extrinsically caused defects. From that, we conclude that the small magnetic part of the relaxation in SrTiO_3 was not caused by the beam implantation.

V. CONCLUSIONS

We have measured the ratio between $1/T_1$ of ^9Li and ^8Li in Pt and SrTiO_3 in order to help identify the nature of the fluctuations responsible for the spin relaxation (i.e., if they are magnetic or electric quadrupolar). In Pt, the relaxation is a single exponential and the ratio R_{Pt} was found to be very close to but slightly less than the pure magnetic limit. This is consistent with Korringa relaxation being dominant, as suggested by the linear temperature dependence in $1/T_1$

reported previously. Nevertheless, the small reduction in R_{Pt} relative to the pure magnetic limit means that excitations causing a fluctuating EFG may provide a small contribution to the observed spin relaxation. Further measurements at lower temperatures would be needed to verify this.

In SrTiO₃ at 300 K the results confirm that the dominant source of relaxation is electric quadrupolar. However, the relaxation function is more complicated, involving a relaxing part and a nonrelaxing part. This suggests there is some inhomogeneous source of fluctuations/spin relaxation, possibly due to nearby defects. The ratio R_{STO} is close to but slightly larger than the pure quadrupolar limit, indicating that there may be some small magnetic contribution. However, the main source of spin relaxation is quadrupolar. This is consistent with expectations given the large quasistatic nuclear quadrupole interaction.

Most importantly, we have demonstrated that the method of isotope comparison can be used in β -NMR to distinguish the nature of the fluctuations responsible for $1/T_1$. This represents an important tool for β -NMR, since in many systems there is uncertainty in the source of relaxation that cannot be removed simply by varying experimental parameters.

ACKNOWLEDGMENTS

We thank TRIUMF's Centre for Molecular and Materials Science (CMMS) for their technical support. This work was supported by NSERC Discovery Grants to R.F.K. and W.A.M. and IsoSiM fellowships to A.C. and R.M.L.M. TRIUMF receives federal funding via a contribution agreement with the Natural Sciences and Engineering Research Council of Canada.

-
- [1] W. A. MacFarlane, *Solid State Nucl. Magn. Reson.* **68–69**, 1 (2015).
- [2] C. D. P. Levy, M. R. Pearson, R. F. Kiefl, E. Mané, G. D. Morris, and A. Voss, *Hyperfine Interact.* **225**, 165 (2014).
- [3] G. D. Morris, *Hyperfine Interact.* **225**, 173 (2014).
- [4] S. Lee, *Solid State Nucl. Magn. Reson.* **71**, 1 (2015).
- [5] P. Bakulé and E. Morenzoni, *Contemp. Phys.* **45**, 203 (2004).
- [6] M. D. Hossain, H. Saadaoui, T. J. Parolin, Q. Song, D. Wang, M. Smadella, K. H. Chow, M. Egilmez, I. Fan, R. F. Kiefl, S. R. Kreitzman, C. D. P. Levy, G. D. Morris, M. R. Pearson, Z. Salman, and W. A. MacFarlane, *Physica B* **404**, 914 (2009).
- [7] J. Koringa, *Physica* **16**, 601 (1950).
- [8] Z. Salman, O. Ofer, M. Radovic, H. Hao, M. Ben Shalom, K. H. Chow, Y. Dagan, M. D. Hossain, C. D. P. Levy, W. A. MacFarlane, G. M. Morris, L. Patthey, M. R. Pearson, H. Saadaoui, T. Schmitt, D. Wang, and R. F. Kiefl, *Phys. Rev. Lett.* **109**, 257207 (2012).
- [9] I. Tomeno and M. Oguchi, *J. Phys. Soc. Jpn.* **67**, 318 (1998).
- [10] O. Ofer, K. H. Chow, I. Fan, M. Egilmez, T. J. Parolin, M. D. Hossain, J. Jung, Z. Salman, R. F. Kiefl, C. D. P. Levy, G. D. Morris, M. R. Pearson, H. Saadaoui, Q. Song, D. Wang, and W. A. MacFarlane, *Phys. Rev. B* **86**, 064419 (2012).
- [11] R. B. Firestone and V. S. Shirley, *Table of Isotopes*, 8th ed. (Wiley, New York, 1996).
- [12] A. Abragam, *Principles of Nuclear Magnetism* (Oxford University Press, Oxford, U.K., 1983).
- [13] N. J. Stone, *At. Data Nucl. Data Tables* **90**, 75 (2005).
- [14] X. Fléchar, E. Liénard, O. Naviliat-Cuncic, D. Rodríguez, M. A. G. Alvarez, G. Ban, B. Carniol, D. Etasse, J. M. Fontbonne, A. M. Lallena, and J. Praena, *Phys. Rev. C* **82**, 027309 (2010).
- [15] D. Borremans, D. L. Balabanski, K. Blaum, W. Geithner, S. Gheysen, P. Himpe, M. Kowalska, J. Lassen, P. Lievens, S. Mallion, R. Neugart, G. Neyens, N. Vermeulen, and D. Yordanov, *Phys. Rev. C* **72**, 044309 (2005).
- [16] A. Voss, M. R. Pearson, J. Billowes, F. Buchinger, K. H. Chow, J. E. Crawford, M. D. Hossein, R. F. Kiefl, C. D. P. Levy, W. A. MacFarlane, E. Mané, G. D. Morris, T. J. Parolin, H. Saadaoui, Z. Salman, M. Smadella, Q. Song, and D. Wang, *J. Phys. G: Nucl. Part. Phys.* **38**, 075102 (2011).
- [17] D. E. Alburger and D. H. Wilkinson, *Phys. Rev. C* **13**, 835 (1976).
- [18] ISAC Yield Database, <http://mis.triumf.ca/science/planning/yield/beam>.
- [19] G. D. Morris, W. A. MacFarlane, K. H. Chow, Z. Salman, D. J. Arseneau, S. Daviel, A. Hatakeyama, S. R. Kreitzman, C. D. P. Levy, R. Poutissou, R. H. Heffner, J. E. Elenewski, L. H. Greene, and R. H. Kiefl, *Phys. Rev. Lett.* **93**, 157601 (2004).
- [20] W. A. MacFarlane, C. D. P. Levy, M. R. Pearson, T. Buck, K. H. Chow, A. N. Hariwal, R. F. Kiefl, F. H. McGee, G. D. Morris, and D. Wang, *J. Phys.: Conf. Ser.* **551**, 012059 (2014).
- [21] W. A. MacFarlane, G. D. Morris, K. H. Chow, R. A. Baartman, S. Daviel, S. R. Dunsiger, A. Hatakeyama, S. R. Kreitzman, C. D. P. Levy, R. I. Miller, K. M. Nichol, R. Poutissou, E. Dumont, L. H. Greene, and R. F. Kiefl, *Physica B* **326**, 209 (2003).
- [22] I. Fan, K. H. Chow, T. J. Parolin, M. Egilmez, M. D. Hossain, J. Jung, T. A. Keeler, R. F. Kiefl, S. R. Kreitzman, C. D. P. Levy, R. Ma, G. D. Morris, M. R. Pearson, H. Saadaoui, Z. Salman, M. Smadella, Q. Song, D. Wang, M. Xu, and W. A. MacFarlane, *Physica B* **404**, 906 (2009).
- [23] O. Ofer, K. H. Chow, I. Fan, M. Egilmez, T. J. Parolin, M. D. Hossain, J. Jung, Z. Salman, R. F. Kiefl, C. D. P. Levy, G. D. Morris, M. R. Pearson, H. Saadaoui, Q. Song, D. Wang, and W. A. MacFarlane, *Phys. Proc.* **30**, 156 (2012).
- [24] W. A. MacFarlane, G. D. Morris, T. R. Beals, K. H. Chow, R. A. Baartman, S. Daviel, S. R. Dunsiger, A. Hatakeyama, S. R. Kreitzman, C. D. P. Levy, R. I. Miller, K. M. Nichol, R. Poutissou, and R. F. Kiefl, *Physica B* **326**, 213 (2003).
- [25] T. J. Parolin, Z. Salman, J. Chakhalian, Q. Song, K. H. Chow, M. D. Hossain, T. A. Keeler, R. F. Kiefl, S. R. Kreitzman, C. D. P. Levy, R. I. Miller, G. D. Morris, M. R. Pearson, H. Saadaoui, D. Wang, and W. A. MacFarlane, *Phys. Rev. Lett.* **98**, 047601 (2007).
- [26] Z. Salman, A. I. Mansour, K. H. Chow, M. Beaudoin, I. Fan, J. Jung, T. A. Keeler, R. F. Kiefl, C. D. P. Levy, R. C. Ma, G. D. Morris, T. J. Parolin, D. Wang, and W. A. MacFarlane, *Phys. Rev. B* **75**, 073405 (2007).
- [27] T. J. Parolin, Z. Salman, K. H. Chow, Q. Song, J. Valiani, H. Saadaoui, A. O'Halloran, M. D. Hossain, T. A. Keeler, R. F.

- Kiefl, S. R. Kreitzman, C. D. P. Levy, R. I. Miller, G. D. Morris, M. R. Pearson, M. Smadella, D. Wang, M. Xu, and W. A. MacFarlane, *Phys. Rev. B* **77**, 214107 (2008).
- [28] D. Wang, Z. Salman, K. H. Chow, I. Fan, M. D. Hossain, T. A. Keeler, R. F. Kiefl, C. D. P. Levy, A. I. Mansour, G. D. Morris, M. R. Pearson, T. J. Parolin, H. Saadaoui, M. Smadella, Q. Song, and W. A. MacFarlane, *Physica B* **404**, 920 (2009).
- [29] T. J. Parolin, J. Shi, Z. Salman, K. H. Chow, P. Dosanjh, H. Saadaoui, Q. Song, M. D. Hossain, R. F. Kiefl, C. D. P. Levy, M. R. Pearson, and W. A. MacFarlane, *Phys. Rev. B* **80**, 174109 (2009).
- [30] K. H. Chow, A. I. Mansour, I. Fan, R. F. Kiefl, G. D. Morris, Z. Salman, T. Dunlop, W. A. MacFarlane, H. Saadaoui, O. Mosendz, B. Kardasz, B. Heinrich, J. Jung, C. D. P. Levy, M. R. Pearson, T. J. Parolin, D. Wang, M. D. Hossain, Q. Song, and M. Smadella, *Phys. Rev. B* **85**, 092103 (2012).
- [31] Z. Salman, R. F. Kiefl, K. H. Chow, W. A. MacFarlane, S. R. Kreitzman, D. J. Arseneau, S. Daviel, C. D. P. Levy, Y. Maeno, and R. Poutissou, *Physica B* **374–375**, 468 (2006).
- [32] Z. Salman, R. F. Kiefl, K. H. Chow, M. D. Hossain, T. A. Keeler, S. R. Kreitzman, C. D. P. Levy, R. I. Miller, T. J. Parolin, M. R. Pearson, H. Saadaoui, J. D. Schultz, M. Smadella, D. Wang, and W. A. MacFarlane, *Phys. Rev. Lett.* **96**, 147601 (2006).
- [33] M. Smadella, Z. Salman, K. H. Chow, M. Egilmez, I. Fan, M. D. Hossain, R. F. Kiefl, S. Kreitzman, C. Levy, W. MacFarlane, A. I. Mansour, G. D. Morris, T. J. Parolin, M. Pearson, H. Saadaoui, Q. Song, and D. Wang, *Physica B* **404**, 924 (2009).
- [34] Z. Salman, M. Smadella, W. A. MacFarlane, B. D. Patterson, P. R. Willmott, K. H. Chow, M. D. Hossain, H. Saadaoui, D. Wang, and R. F. Kiefl, *Phys. Rev. B* **83**, 224112 (2011).
- [35] Bulk LaTiO_3 is a prototypical Mott insulator and is antiferromagnetic below ~ 135 K. As SrTiO_3 , LaTiO_3 is nonmagnetic at 300 K, though transport measurements have shown the existence of a metallic and superconducting heterointerface.
- [36] J. F. Ziegler, M. D. Ziegler, and J. P. Biersack, *Nucl. Instrum. Methods Phys. Res., Sect. B* **268**, 1818 (2010).
- [37] Z. Salman, E. P. Reynard, W. A. MacFarlane, K. H. Chow, J. Chakhalian, S. R. Kreitzman, S. Daviel, C. D. P. Levy, R. Poutissou, and R. F. Kiefl, *Phys. Rev. B* **70**, 104404 (2004).